



Using the Biotic Ligand Model framework to investigate binary metal interactions on the uptake of Ag, Cd, Cu, Ni, Pb and Zn in the freshwater snail *Lymnaea stagnalis*



Anne Crémazy^{a,*}, Kevin V. Brix^b, Chris M. Wood^a

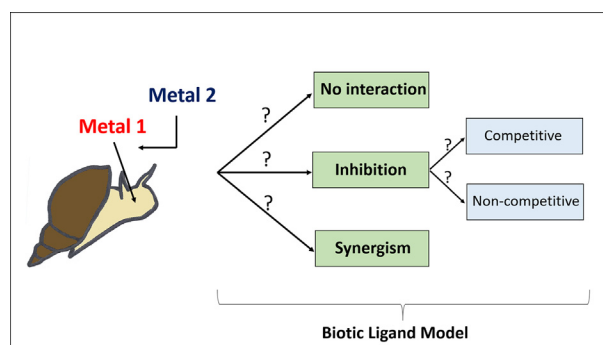
^a Department of Zoology, University of British Columbia, Vancouver, BC V6T 1Z4, Canada

^b University of Miami, RSMAS, Miami, FL, USA

HIGHLIGHTS

- The uptake of 6 metals alone and in binary combinations were measured in snails.
- The BLM framework was used to evaluate single metal uptake and binary interactions.
- Most interactions were inhibitory, relatively small, and not reciprocal.
- Most of the interactions could be explained via competitive interactions.
- This study shows the potential of the BLM to predict metal mixtures bioaccumulation.

GRAPHICAL ABSTRACT



ARTICLE INFO

Article history:

Received 4 July 2018

Received in revised form 30 July 2018

Accepted 31 July 2018

Available online 1 August 2018

Editor: Shuzhen Zhang

Keywords:

Lymnaea stagnalis

Metal mixtures

Short-term uptake

Biotic Ligand Model

ABSTRACT

There is growing interest in the development of mechanistically-based models, such as the Biotic Ligand Model (BLM), for assessing the environmental risk of metal mixtures. However, the derivation of such models requires insights into the mechanisms of multimetal interactions that are often lacking for aquatic organisms. In the present study, we investigated how binary mixtures of six metals (Ag, Cd, Cu, Ni, Pb and Zn) interact for uptake in the great pond snail *Lymnaea stagnalis*, a freshwater species particularly sensitive to metals in chronic exposure. For each metal, short-term (2–3 h) uptake experiments on juvenile snails were performed with the metal alone and in combination with a second metal, at concentrations encompassing the chronic toxicity concentration range. These experiments showed significant binary metal interactions for 7 out of 15 mixtures. Most interactions were inhibitory in nature, not reciprocal and caused by either Ag or Cu. They led to relative changes of uptake that did not exceed 50% within the range of metal chronic toxicity. The BLM proved to be successful at explaining most of the interactions, via competitive inhibition. This study is in support of using bioavailability-based models, such as the BLM, to model metal mixture interactions in *L. stagnalis*.

© 2018 Published by Elsevier B.V.

1. Introduction

While metals invariably occur in mixtures in the environment, ecological risk assessments still mostly rely on effects evaluations obtained for single elements. Incorporating metal mixtures into regulatory

* Corresponding author at: Department of Zoology, University of British Columbia, 6270 University Blvd, Vancouver, BC V6T 1Z4, Canada.

E-mail address: anne.cremazy@gmail.com (A. Crémazy).

frameworks has been an important focus of environmental scientists and regulators over the past decade (Meyer et al., 2015; Van Genderen et al., 2015). An often-used approach in mixture regulation is the use of additive models, such as the Concentration Addition (CA) and Independent Action (IA) models, which predict mixture toxicity based on the toxicity of each mixture component, without consideration of their potential interactions (Backhaus and Faust, 2012). Yet, it is well recognised that metals can affect one another's toxicity and that overlooking their joint effects may lead to erroneous toxicity prediction and *in fine* risk assessment. Indeed, metal mixture toxicity to aquatic organisms has often been shown to deviate from strict additivity, most often in a less-than-additive manner, although more-than-additive interactions are also occasionally observed (Vijver et al., 2011; Norwood et al., 2003). Different approaches have recently been proposed to start accounting for multi-metal interactions in mixture toxicity evaluation. Among them, bioavailability-based models, such as the Biotic Ligand Model (BLM), offer a conceptual framework viewed as rather suitable for metal mixtures assessment (Balistriero and Mebane, 2014; Iwasaki et al., 2015; Santore and Ryan, 2015). Briefly, within the BLM framework, metal bioavailability is proportional to the amount of metal chemically bound to sensitive biological sites referred to as "biotic ligands" (BL, e.g. membrane ion transporters), which are modulated by the presence of (i) the major cations in solution competing with the metal for binding to the BL (e.g. H^+ , Ca^{2+} , Na^+) and (ii) the abiotic ligands in solution competing with the BL for binding to the metal (e.g. SO_4^{2-} , Cl^- , dissolved organic matter (DOM)). While this model is a simplification of complex processes in metal toxicity, the general success of the BLM in predicting metal toxicity under different water chemistries represents a major progress in metal risk assessment (Di Toro et al., 2001; Paquin et al., 2002; Niyogi and Wood, 2004; Ardestani et al., 2014). Diverse adaptations of the BLM have been proposed to account for multiple metal interactions (Balistriero and Mebane, 2014; Balistriero et al., 2015; Farley and Meyer, 2015; Iwasaki et al., 2015; Santore and Ryan, 2015). In these multi-metal BLMs, metal-metal interactions are described as competitive binding for abiotic and biotic ligands. For example, inhibition on metal uptake may be explained as competition for the same metal transporter at the biological surface. On the other hand, increased metal uptake may be explained by the displacement of metal bound to an aqueous ligand (e.g. DOM) by another metal, leading to increased free metal concentration (and thus bioavailability) of the first metal. Yet, one major hurdle for the development of such mechanistic models is the lack of experimental data on how multiple metals interact at sites of uptake and toxicity (i.e., at BLs). This critical need for more metal mixture data has notably been highlighted by recent studies showing that multi-metal interactions appear to be species-specific and do not always match theoretical predictions from current toxicological knowledge (Pelgrom et al., 1995; Komjarova and Blust, 2009; Niyogi et al., 2015; Brix et al., 2017). The lack of experimental studies is even greater for chronically metal-sensitive organisms, in contrast to acutely metal-sensitive organisms (Meyer et al., 2015; Van Genderen et al., 2015; Nys et al., 2017). The current work is a direct response to this data gap.

In the present study, we investigated how six trace metals (Ag, Cd, Cu, Ni, Pb and Zn) interact with each other for short-term uptake in the great pond snail *Lymnaea stagnalis*. This pulmonate freshwater mollusc was selected for its high sensitivity to several metals in chronic exposures, making it a very relevant species in metal risk assessment. Indeed, it has been shown to be one of the most chronically sensitive freshwater organisms to Ag, Co, Cu, Ni and Pb, with inhibitory effects on growth and reproduction (De Schampelaere et al., 2008; Brix et al., 2011; Brix et al., 2012; Niyogi et al., 2014; Crémazy et al., 2018). As for most aquatic organisms, chronic metal toxicity to *L. stagnalis* seems to be regulated by water chemistry in accordance with the BLM (De Schampelaere and Janssen, 2010; Schlekot et al., 2010; Esbaugh et al., 2012), and has been proposed to be associated with impairment of ionoregulation (more precisely of Ca homeostasis) (Grosell and

Brix, 2009; De Schampelaere and Janssen, 2010; Brix et al., 2011). We have recently observed that binary mixtures of the six metals presently studied elicited a great proportion of less-than-additive responses in chronic toxicity to *L. stagnalis* (Crémazy et al., 2018). The present work aims at providing some potential mechanistic insights on these previous observations. Specifically, this study focuses on characterizing binary metal interactions occurring at the first step of metal toxicity: uptake into the organism. To do so, short-term metal internalization fluxes were measured in juvenile snails, using radio-isotopes as tracers (except for Pb). These fluxes were obtained for metals present alone and in combination with a second non-labelled metal, at concentrations ranges where chronic toxicity was previously observed (Crémazy et al., 2018). The BLM mathematical framework was used to analyze the uptake dataset and to characterize the types of binary metal interactions occurring. We hypothesized that most interactions on uptake would be inhibitory in nature, as is usually the case for metal mixtures (Norwood et al., 2003; Vijver et al., 2011), and notably for our parallel chronic toxicity study on this species (Crémazy et al., 2018). We also hypothesized that the BLM could explain most of the interactions i) *via* metal-metal competition for abiotic ligands in solution (enhanced uptake) and ii) *via* metal-metal competition for membrane transporters (reduced uptake).

2. Materials and methods

2.1. Experimental animals and water composition

The culture conditions of *L. stagnalis* were the same as previously described in Crémazy et al. (2018). The snails were kept at $25 \pm 1^\circ C$, under a 16 h light:8 h dark photoperiod, in Vancouver dechlorinated tap water (from the Capilano watershed) amended with salts to promote healthy snail growth. This water was used both for snail culture and for the uptake tests conducted in this study. Its composition, as measured during these tests, was: $pH = 7.85 \pm 0.20$, $[Ca] = 0.99 \pm 0.01$ mM, $[Mg] = 0.22 \pm 0.02$ mM, $[Na] = 1.7 \pm 0.2$ mM, $[K] = 0.054 \pm 0.015$ mM, $[Cl] = 1.0$ mM (nominal), $[SO_4] = 0.79$ mM (nominal), $[dissolved\ organic\ carbon, DOC] = 0.80 \pm 0.08$ mg·L⁻¹, alkalinity = 0.80 ± 0.05 mEq·L⁻¹ (measured as [dissolved inorganic carbon]) and hardness = 120 mg·L⁻¹ as CaCO₃. The culture was kept under static renewal conditions and was fed a mix of thoroughly washed, peeled sweet potato (*Ipomoea batatas*) and romaine lettuce (*Lactuca sativa*).

2.2. Short-term metal uptake tests

Short-term metal uptake experiments were carried out with juvenile snails (about 3 weeks old, ca. 150 mg whole wet weight). They were starved for 24 h prior to the tests. For each treatment, one snail was exposed in 45 mL of aerated exposure solution, in 50 mL polypropylene tubes. Note that the high water volume-to-snail ratio and short exposure time facilitated constant water physico-chemistry throughout the tests. These solutions were prepared 24 h prior to the experiment, in order to allow for thermodynamic equilibrium to be reached. The water was the same as for snail culture (see composition in Section 2.1), with the addition of the appropriate metal salt(s) (AgNO₃, CdCl₂·5H₂O, CuCl₂·2H₂O, NiCl₂·6H₂O, Pb(NO₃)₂, Zn(NO₃)₂·6H₂O, ACS grade, Fisher Scientific). Additionally, in order to trace Ag, Cd, Cu, Ni and Zn uptake in the snails at relatively low concentrations, the tests solutions were spiked with the appropriate amount of radioisotope: Ag-110 m (as AgNO₃, experimental specific activity (SpA) ~50 Ci·mol⁻¹, Eckert and Ziegler, Valencia, CA, USA), Cd-109 (as CdCl₂, SpA ~10 Ci·mol⁻¹, Eckert and Ziegler, Valencia, CA, USA), Cu-64 (as CuCl₂, SpA ~500 Ci·mol⁻¹, TRIUMF, Vancouver, Canada), Ni-63 (as NiCl₂, SpA ~10 Ci·mol⁻¹, Eckert and Ziegler, Valencia, CA, USA) and Zn-65 (as ZnCl₂, SpA ~1 Ci·mol⁻¹, PerkinElmer, Toronto, Canada). Because of the high specific activities, the added radioactivity had negligible effect on the total exposure concentrations. No suitable radio-isotope was available for Pb, so this metal

was not radiolabelled in the tests. At the beginning and at the end of each uptake test, water samples were collected from each test vial and filtered (0.45 µm polyethersulfone membrane, Membrane Solution, Dallas, TX, USA) for subsequent water analyses (as described in Section 2.3.1). At the end of each uptake test, a 3-step snail rinsing procedure was implemented to ensure desorption of surface-bound metal, and that only internalized metal was measured in the snail tissues. First, snails were briefly rinsed with a rinsing solution corresponding to the exposure solution without metal. Second, they were exposed for 5 min in 20 mL of either 10 mM sodium thiosulfate ($\text{Na}_2\text{S}_2\text{O}_3 \cdot 5\text{H}_2\text{O}$, ACS grade, Fisher Scientific) for Ag uptake tests, or 1 mM ethylenediaminetetraacetic ($\text{EDTA} \cdot 2\text{H}_2\text{O}$, ACS grade Fisher Scientific) for the other metals uptake tests. Third, the first step was repeated and snails were blotted dry on a tissue paper and kept frozen at -20°C until subsequent tissue analysis (as described in Section 2.3.2).

Four sets of uptake experiments were carried out in this study, using the above protocol. In a first set of experiments, the uptake of each metal in the snail's soft tissues (corresponding to the whole snail without shells and digestive tracts) was characterized as a function of time. This was done by measuring individual radiolabelled metal uptake at four exposure times between 0.5 and 4 h, at one metal concentration. We selected toxicologically relevant metal concentrations of 0.1 µM Ag, 0.2 µM Cd, 0.1 µM Cu, 5 µM Ni, 0.4 µM Pb and 3 µM Zn. For Cd, Cu, Pb and Ni, these concentrations were indeed very close to the effect concentration leading to 50% inhibition of growth rate measured in previously performed 14-d chronic toxicity tests (14-d EC50 = 0.2 µM Cd, 0.1 µM Cu, 4 µM Ni, 6 µM Zn, Crémazy et al., 2018). For Ag and Pb, the selected concentrations were respectively about 5 and 4 times their previously measured 14-d EC50 values (0.02 µM Ag and 0.1 µM Pb), for signal detection reasons. Each test was performed in triplicate ($n = 3$). This first set of preliminary tests allowed checking that influx was linear with time, and that the rinsing procedure was effective at removing surface-bound metals (see Results).

In a second set of experiments, the tissue-specific distribution of each metal in *L. stagnalis* was characterized after a 2-h exposure to each individual radiolabelled metal and a 3-h exposure to Pb (for signal sensitivity reasons), at the same metal concentrations as given above, with $n = 6$ for each exposure. For these tests, metal accumulation was measured in the digestive tract (with chyme), the foot, the mantle and in a last fraction combining the rest of the soft tissues. These tests aimed at determining if one of these specific tissues accumulated more than the other, or if uptake occurred indiscriminately across the whole integument. Based on the results, metal uptake was subsequently analyzed in the whole soft tissues without the digestive tract (simply referred to as "soft tissues" in the remainder of the manuscript).

In a third set of experiments, the 2-h (3-h for Pb) uptake profiles of radiolabelled metals in the soft tissues were characterized within the following concentration ranges: 0.0005–0.2 µM Ag, 0.03–4 µM Cd, 0.007–0.3 µM Cu, 0.02–5 µM Ni, 0.03–0.4 µM Pb and 0.6–20 µM Zn (see details in Table SI.1 of the Supporting information). Each treatment was performed in triplicate ($n = 3$). These latter ranges encompassed the "chronic concentration ranges", defined in this paper as the metal concentration ranges where 0–100% inhibition of snail growth rate were previously observed in 14-d chronic toxicity tests (Crémazy et al., 2018). These chronic concentration ranges were 0–0.08 µM Ag, 0–0.4 µM Cd, 0–0.3 µM Cu, 0–4 µM Ni, 0–0.4 µM Pb and 0–10 µM Zn.

In a last set of experiments, we observed the effects of non-radiolabelled secondary metals (Ag, Cd, Cu, Ni, Pb or Zn) on the 2-h soft tissue uptake of a primary radiolabelled metal (or 3-h soft tissue uptake of cold Pb). In these experiments, the primary metal was held constant at two concentrations around the 14-d EC20 and 14-d EC90 values (Crémazy et al., 2018), while the secondary metal concentration was increased in a range encompassing its chronic toxicity range (see details in Table SI.2). Each treatment was performed in triplicate ($n = 3$).

2.3. Sample analyses

2.3.1. Exposure water

Non-radioactive inorganic elements were analyzed in the filtered water samples by atomic absorption spectrometry (AA240 FS, Varian) with a graphite furnace for Ag, Cd, Cu, Pb and Ni and with a flame for Zn, Ca, Mg, K and Na. Dissolved organic carbon (DOC) concentrations were measured with a Total Organic Carbon analyzer (V-series TOC analyzer, Shimadzu). The pH was measured with an Orion™ Green pH combination electrode (Fisher Scientific). Trace metal concentrations were measured in all water samples collected, i.e. in all test solutions at the start and end of the uptake period. On the other hand, the pH and major cations and DOC concentrations were only measured in 6 random samples for each uptake experiment: 3 at the start and 3 at the end of the uptake period. Instrument calibrations were verified with certified reference waters TMDA-54.5 and TM-25.4 (Natural Resources Canada). Gamma radioactivity of Ag-110 m, Cd-109, Cu-64 and Zn-65 was measured in the different water samples with a gamma counter (Automatic gamma counter, Wallac Wizard Model 1470). The beta radioactivity of Ni-63 was measured in the different water samples with a beta counter (LS 6500, Beckman Coulter) after mixing with scintillation cocktail (Ultima-Gold AB®, PerkinElmer, Toronto, Canada); tests showed that quenching was constant, so no correction was made.

2.3.2. Snail tissues

Test snails were thawed and their tissues were dissected and precisely weighed (± 0.1 mg). The non-radiolabelled Pb concentration was measured by atomic absorption spectrometry (as previously described in Section 2.3.1). The radioactivity of Ag-110, Cd-109, Cu-64 and Zn-65 was directly measured in the intact tissues by gamma counting (as previously described in Section 2.3.1). For beta emitters (Ni-63) and non-radiolabelled metals (Pb) analyses, tissues were first digested in 200 µL of 50% v/v HNO_3 (ACS grade, Fisher Scientific) for 2 days at 65°C . The radioactivity of Ni-63 was then measured by beta counting (as previously described in Section 2.3.1), with quench correction performed using different volumes of acid digests and the external standard method to correct for the counting efficiency difference with that in the water. As quenching in water was constant, tissue counting efficiency was thereby corrected to the same level as water counting efficiency. For Ag, Cd, Cu and Zn, uptake in snails ($\text{nmol} \cdot \text{g}^{-1}$) was calculated based on accumulation of radioactivity in the digested tissue and the specific activity of the radioisotope in the water:

$$M \text{ uptake} = a \cdot (b \cdot c^{-1})^{-1} \quad (1)$$

where a = the $\text{CPM} \cdot \text{g}^{-1}$ of snail tissue (wet weight), b = the $\text{CPM} \cdot \text{mL}^{-1}$ in the water, and c = the measured dissolved metal concentration in the water ($\text{nmol} \cdot \text{mL}^{-1}$).

2.4. Data analyses

2.4.1. Metal aqueous speciation calculations

Measured water physico-chemistry was entered into the Windermere Humic Aqueous Model (WHAM, version VII) to compute the free ion activity of each metal M ($\{M^{z+}\}$, with $z = 1$ or 2) in the different test solutions. The software's default thermodynamic database was unchanged, except for the metal carbonate constants which were replaced by the NIST recommended values (as detailed in Crémazy et al., 2018). Metal complexation with dissolved organic matter (DOM) was modelled using the classical assumption that DOM is composed of 50% carbon by weight (Buffle, 1988) and corresponds to 65% "active" fulvic acid (Bryan et al., 2002).

2.4.2. Uptake data analyses

Uptake data analyses were performed on uptake fluxes (J_{int} , in $\text{nmol} \cdot \text{g} \cdot \text{h}^{-1}$), corresponding to the amount of metal (in nmol) per unit of soft tissue weight (in g of wet weight) per unit of exposure time (in hour). The BLM framework was used to analyze the obtained dataset. As this model stipulates that bioavailability is better predicted by the aqueous free ion metal activity $\{M^{z+}\}$ rather than by the measured total dissolved metal concentration $[M]$, data analysis was based on $\{M^{z+}\}$ (calculated as described in Section 2.4.1),

The single-metal and mixture uptake data were then analyzed by regression, using the SigmaPlot® software. First, for each single-metal uptake test, obtained J_{int} values were modelled at varying $\{M^{z+}\}$ according to the Michaelis-Menten saturation kinetics predicted by the BLM:

$$J_{\text{int}} = \frac{J_{\text{max}} \cdot K_M \cdot \{M^{z+}\}}{1 + K_M \cdot \{M^{z+}\}} \quad (2)$$

The maximal flux J_{max} (in $\text{nmol} \cdot \text{g} \cdot \text{h}^{-1}$) corresponds to the situation where the metal transport system is saturated with substrate. Under equilibrium assumptions, K_M (in M^{-1}) is considered the apparent stability constant between the metal M ($M = \text{Ag}, \text{Cd}, \text{Cu}, \text{Ni}, \text{Pb}$ or Zn) and its membrane transporter. It is equal to the inverse of the Michaelis-Menten parameter K_m (in M) (i.e., $K_M = 1 / K_m$). The value of K_M is conditional on the ionic strength, pH and temperature of the exposure water.

Secondly, for each mixture uptake test, the effect of increasing the secondary metal free ion activity $\{M_2^{z+}\}$ on the primary metal M_1 uptake flux was modelled with Eq. (3), which is an extension of Eq. (2). This modeling was performed at each the two fixed $\{M_1^{z+}\}$ selected in each binary mixture test (c.f. Section 2.3).

$$J_{\text{int},M_1} = \frac{J_{\text{max},M_1} \cdot K_{M_1} \cdot \{M_1^{z+}\}}{1 + K_{M_1} \cdot \{M_1^{z+}\} + K_{M_2} \cdot \{M_2^{z+}\}} \quad (3)$$

where J_{max,M_1} is the maximal flux of M_1 and where K_{M_1} and K_{M_2} respectively are the apparent stability constants of M_1 and M_2 with the membrane transporter of M_1 .

A significant value for K_{M_2} ($p < 0.05$) was interpreted as a significant competitive interaction between M_2 and M_1 for binding to the M_1 membrane transporter. For these modeling runs, the parameter K_{M_1} was set at the value obtained from the single-metal J_{int} modeling with Eq. (2), while J_{max,M_1} and K_{M_2} were the fitting parameters. The parameter J_{max,M_1} was not fixed in order to account for potential physiological changes between the snails used in the different tests. Indeed, physiological changes affecting metal uptake are reflected in changes in J_{max} values. Since the single-metal and mixture uptake tests were not performed simultaneously, physiological differences and thus J_{max} differences were indeed possible. Additionally, a significant shift in J_{max} between the two selected $\{M_1^{z+}\}$ values may indicate a non-competitive type of interaction between M_1 and M_2 .

2.4.3. Statistical analyses

The significance level in this study was set at $\alpha = 0.05$. Comparisons among different tissues' metal contents were performed with an ANOVA followed by a Tukey's HSD test for multiple comparisons. The significance level on each fitted parameter from Eqs. (2) and (3) were given by SigmaPlot®. Changes in J_{max} between $\{M_1^{z+}\}$ for each binary mixture uptake test was assessed with a t -test. Comparison between the different metals' J_{max} and K_M values obtained with Eq. (2) was performed with a t -test with a False Discovery Rate (FDR) correction for multiple comparisons.

3. Results

Within the short time range of the uptake tests, the variation of the measured water physico-chemistry parameters was $<20\%$. The mean

physico-chemistry parameters are given in Section 2.1 of the Materials and methods.

For each metal, individual metal uptake in the snail soft tissues increased linearly over the short exposure times used in this study (Fig. SI.1 in the Supporting information), indicating no detectable backflux of the radioisotope (or cold Pb). Linear regressions of these relationships showed y-intercepts which were not significantly different from zero ($p > 0.05$), which, according to the classical interpretation of uptake kinetic data, implies that only internalized metal and not adsorbed metal was measured in the snails (Hassler et al., 2004). It also indicates that the different rinsing procedures employed in this study were efficient at removing surface-bound metals and/or that this latter fraction was negligible compared to the internalized metal fraction. These different observations on metal uptake kinetics confirmed that we were measuring internalization fluxes in our short-term uptake tests.

3.1. Silver uptake

In the exposures with Ag only, Ag accumulated preferentially in the foot and the mantle, with the lowest accumulation observed in the digestive tract (Fig. 1A). According to WHAM VII, the free Ag^+ represented 31% of the total dissolved Ag species (based on activity) in the single-metal uptake tests (Table SI.1). The most important chemical species was AgCl and the proportion of Ag bound to DOM was around 1%. The measured Ag J_{int} values were linear with $\{\text{Ag}^+\}$, as no sign of uptake saturation was observed (Fig. 2A). This profile corresponds to a specific case of Eq. (2) where $K_M \cdot [M^{z+}] \ll 1$, so that Eq. (2) can be simplified to the linear equation: $J_{\text{int}} = J_{\text{max}} \cdot K_M \cdot [M^{z+}]$. Hence, only the slope $J_{\text{max}} \cdot K_{\text{Ag}}$ could be obtained from the regression of these single Ag uptake tests (see footnote of Table 1). However, the Ag uptake profile allowed us to estimate minimum values for J_{max} ($>6 \text{ nmol} \cdot \text{g}^{-1} \cdot \text{h}^{-1}$) and K_{Ag} ($>10^{7.3} \text{ M}^{-1}$) (Table 1). When expressed as a function of total dissolved concentration, the apparent K_{Ag} value was $>10^{6.8} \text{ M}^{-1}$ (see Table SI.3).

In the mixture exposures, the WHAM VII calculations suggest that the proportion of Ag^+ in solution was unaffected by the presence of a second metal (Table SI.2). Cadmium, Ni, Pb and Zn had no effect on Ag J_{int} values (Fig. 2B, D, E, F), with no changes in $J_{\text{max},\text{Ag}}$ (between each $\{\text{Ag}^+\}$ tested) and no significant K_{M_2} being observed from data fitting with Eq. (3) (Table 2). Only Cu seemed to affect Ag uptake fluxes in *L. stagnalis*, but in a way that did not follow BLM predictions (Fig. 2C). Indeed, at both selected $\{\text{Ag}^+\}$ levels, Cu firstly enhanced (by up to 2-fold at 2 nM Cu^{2+}) then inhibited Ag uptake in *L. stagnalis*. No significant K_{M_2} could be derived from these curves (Table 2). The overall effect of Cu on Ag J_{int} , depicted in Fig. 2C, was a 70% decrease within the tested concentration range ($0\text{--}9 \text{ nM Cu}^{2+}$) and a 60% decrease within the Cu chronic concentration range ($0\text{--}6 \text{ nM Cu}^{2+}$).

3.2. Cadmium uptake

In the exposures with Cd only, Cd was around 4-times more concentrated in the digestive tract than in the rest of soft tissues analyzed, which did not show any differential Cd burden (Fig. 1B). According to the WHAM VII calculations for the Cd only uptake tests, the free Cd^{2+} was the most important of the dissolved species (57%, based on activity), followed by the sulfato- and DOM-complexes (around 10%), then by the carbonato- and chloro-complexes (around 5%) (Table SI.1). The Cd J_{int} values measured in the soft tissues of *L. stagnalis* showed a Michaelis-Menten type of relationship with $\{\text{Cd}^{2+}\}$ (Fig. 3A). The corresponding estimated J_{max} was $41 \text{ nmol} \cdot \text{g}^{-1} \cdot \text{h}^{-1}$ and the apparent K_{Cd} was $10^{5.6} \text{ M}^{-1}$ (Table 1). When the analysis was based on total dissolved concentration rather than free ion activity, the K_{Cd} value slightly decreased to $10^{5.3} \text{ M}^{-1}$ (Table SI.3).

In the mixture exposures, the WHAM VII calculations suggest that the proportion of Cd^{2+} in solution was negligibly affected by the

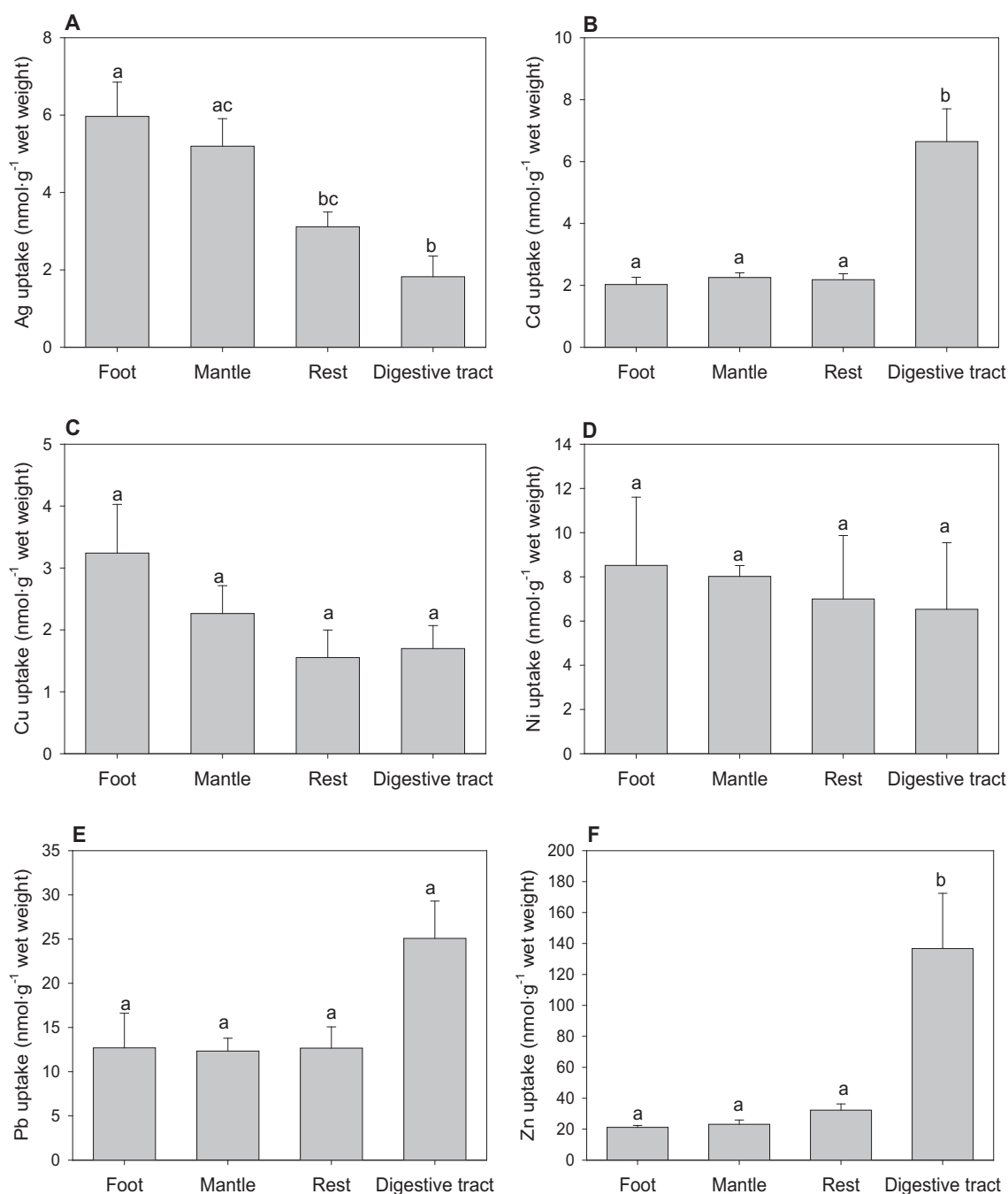


Fig. 1. Concentration of A) Ag, B) Cd, C) Cu, D) Ni, E) Pb and F) Zn in the foot, the mantle, the rest of the soft tissues and the digestive tract (with chyme) of *L. stagnalis* exposed for 2 h (3 h for Pb). Water exposure concentrations were 0.1 μM Ag, 0.2 μM Cd, 0.1 μM Cu, 5 μM Ni, 0.4 μM Pb and 3 μM Zn. Values are mean \pm SE ($n = 6$). Comparisons between tissues are performed with a one-way ANOVA with a Tukey test ($\alpha = 0.05$). Estimates not sharing common letters are significantly different.

presence of a second metal in solution (Table SI.2). Nickel, Pb and Zn had no effect on Cd uptake in *L. stagnalis* (Fig. 3D, E, F and Table 2), but Ag and Cu both inhibited Cd uptake fluxes in a manner that could be captured by the BLM (Fig. 3B, C and Table 2). Indeed, fitting Cd J_{int} with Eq. (3) provided conditional affinity constants of Ag and Cu for the Cd transporter: the K_{Ag} was calculated at $10^{7.7-7.6} \text{ M}^{-1}$ (at low and high Cd concentrations), while the K_{Cu} was calculated at $10^{8.2-8.1} \text{ M}^{-1}$ (at low and high Cd concentrations). On the other hand, no apparent effect of these secondary metals was observed on $J_{\text{max,Cd}}$. Overall, the effects on Cd J_{int} were a 70% decrease within the tested Ag and Cu concentration ranges (0–50 nM Ag^+ and 0–11 nM Cu^{2+}) and a 50% decrease within the Ag and Cu chronic concentration ranges (0–30 nM Ag^+ and 0–6 nM Cu^{2+}).

3.3. Copper uptake

In the exposures with Cu only, Cu was equally accumulated in the different snail tissues (Fig. 1C). For the Cu-alone uptake tests, the proportion of free Cu^{2+} in solution varied from 0.18 to 3.5% (based on activity) within the range of the total dissolved Cu concentration tested. Indeed, WHAM VII predicted a gradual occupancy of the finite number of DOM binding sites with the increase of total aqueous Cu, with the proportion of Cu-DOM decreasing from 98 to 56%. The measured Cu J_{int} in the soft tissues of *L. stagnalis* showed a Michaelis-Menten type of relationship with $\{\text{Cu}^{2+}\}$ (Fig. 4A). The estimated J_{max} was $2.5 \text{ nmol}\cdot\text{g}^{-1}\cdot\text{h}^{-1}$ and the apparent K_{Cu} was $10^{8.7} \text{ M}^{-1}$ (Table 1).

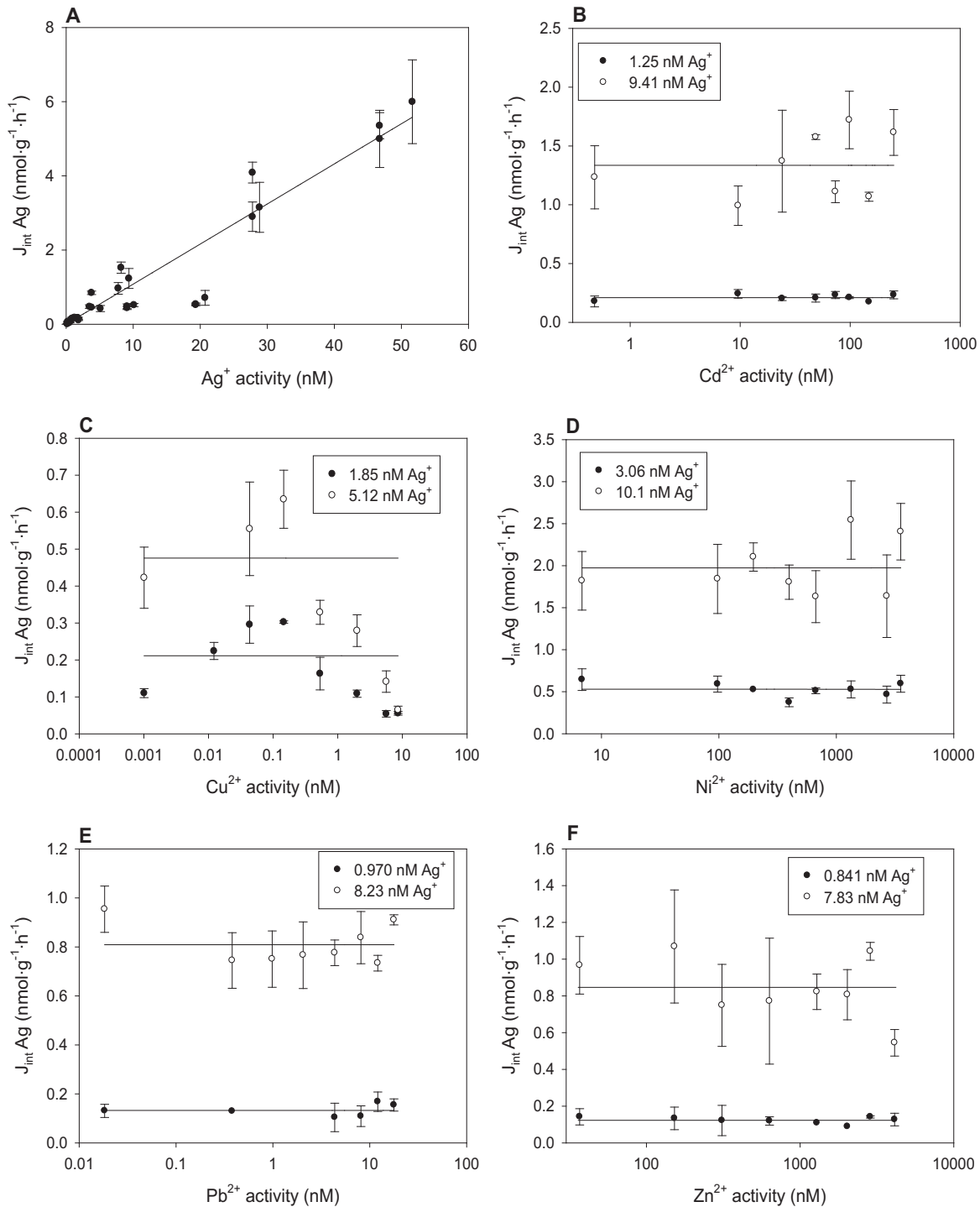


Fig. 2. Internalization flux of Ag in the soft tissues of *L. stagnalis* exposed for 2 h, as a function of the calculated aqueous activity of A) Ag^+ , B) Cd^{2+} , C) Cu^{2+} , D) Ni^{2+} , E) Pb^{2+} and F) Zn^{2+} . Values are mean \pm SE ($n = 3$). Data in panel A were obtained from a single-metal uptake test and are fitted with Eq. (2) (plain line: regression line). Data in panels B, C, D, E and F were obtained from binary mixture tests at two Ag^+ concentrations (white and black circles) and were fitted with Eq. (3) (plain lines: regression lines, with K_{M2} set to 0 when found to be non-significant ($p > 0.05$)).

When the analysis was based on total dissolved concentration, the K_{Cu} value decreased considerably to $10^{6.1} \text{ M}^{-1}$ (Table SI.3).

In the mixture exposures, the WHAM VII calculations suggest that the proportion of Cu^{2+} was significantly increased by the presence of Ni (up to 1.8-fold), Pb (up to 3.4-fold) and Zn in solution (up to 9.5-fold), as a result of multi-metal competition for complexation to the same DOM binding sites (Table SI.2). However, these geochemical effects did not increase Cu uptake (note: regression analyses with Eq. (3) were performed on the mean $\{\text{Cu}^{2+}\}$ values). Indeed, only Ag seemed to affect Cu J_{int} values, in an inhibitory fashion (Fig. 4B). This

inhibition by Ag could be captured by the BLM (Table 2), with a conditional affinity constants of Ag for the Cu transporter of $10^{7.8} \text{ M}^{-1}$ (and no apparent change in $J_{max,Cu}$). The overall effect on Cu J_{int} was a 80% decrease within the tested Ag concentration range (0–80 nM Ag^+) and a 50% decrease within the Ag chronic concentration range (0–30 nM Ag^+).

3.4. Nickel uptake

In the exposures with Ni only, Ni was equally accumulated by the different snail tissues analyzed in this study (Fig. 1D). According to the

Table 1

Summary of the BLM parameters: $\log K_M$ (log of the apparent stability constant between the metal M and its membrane transporter, in M^{-1}) and J_{max} (the maximal uptake flux, in $nmol \cdot g^{-1} \cdot h^{-1}$). These values were obtained by fitting the single-metal uptake kinetics data using estimated free ion concentrations (panels A of Fig. 2 to 7) with Eq. 2. Values are mean estimates with their 95% confidence intervals, except for K_M and J_{max} of Ag where only minimum values could be estimated. For each parameter, comparison between metals was performed with a t-test with a false discovery rate (FDR) correction ($\alpha = 0.05$). Estimates not sharing common letters are significantly different.

	Log K_M	J_{max}	R^2	n
Ag⁺ *	> 7.3	> 6	0.886	32
Cd²⁺	5.6 [n.a.** - 6.0] ^{abcd}	41 [10 - 71] ^a	0.964	9
Cu²⁺	8.7 [7.8 - 8.9] ^a	2.5 [1.7 - 3.4] ^b	0.982	10
Ni²⁺	5.9 [5.3 - 6.1] ^b	3.6 [2.4 - 4.9] ^b	0.961	10
Pb²⁺	8.1 [7.6 - 8.3] ^c	7.7 [4.8 - 11] ^c	0.965	8
Zn²⁺	5.1 [4.6 - 5.4] ^d	32 [21 - 44] ^a	0.960	9

* $\log (J_{max} \cdot K_{Ag}) = 8.0 [8.0 - 8.1]$

** n.a.: not applicable (lower limit <0).

WHAM VII calculations, the proportion of Ni^{2+} was the most important of the dissolved species (58%, based on activity) in the Ni-alone uptake tests. Other significant chemical species were carbonato-, sulfato- and DOM-complexes. Nickel uptake fluxes in the soft tissues of *L. stagnalis* showed a Michaelis-Menten type of relationship as a function of $\{Ni^{2+}\}$ (Fig. 5A). The estimated J_{max} was $3.6 nmol \cdot g^{-1} \cdot h^{-1}$ and the apparent K_{Ni} was $10^{5.9} M^{-1}$ (Table 1). When the analysis was based on total dissolved concentration, the K_{Ni} value slightly decreased to $10^{5.6} M^{-1}$ (Table SI.3).

Table 2

Summary of the BLM parameters obtained by fitting the binary metal mixture uptake data (panels B to F of Fig. 2 to 7) with Eq. 3 for each concentration of the primary metal M_1 . Parameters are $J_{max, M1}$ (maximal uptake flux of M_1 , in $nmol \cdot g^{-1} \cdot h^{-1}$) and $\log K_{M2}$ (log of stability constant between the metal M_2 and the membrane transporter of M_1 , in M^{-1}), except for Ag where $\log (J_{max, M1} \cdot K_{M1})$ is given instead of $J_{max, M1}$. Values are mean with their 95% confidence intervals, except for non-significant parameters where $p > 0.05$ is indicated. For each parameter, a significant difference between the two M_1 concentrations are indicated with an asterisk * (t-test, $\alpha = 0.05$).

M_1	M_2	$J_{max, M1}$ (for Cd, Cu, Ni, Pb, Zn)		$\log K_{M2}$	
		$\log (J_{max, M1} \cdot K_{M1})$ (for Ag)			
		Low [M_1]	High [M_1]	Low [M_1]	High [M_1]
Ag	Cd	8.2 [7.8 - 8.4]	8.2 [7.7 - 8.4]	$p > 0.05$	$p > 0.05$
	Cu	8.1 [7.6 - 8.3]	8.0 [7.5 - 8.3]	$p > 0.05$	$p > 0.05$
	Ni	8.2 [8.8 - 8.5]	8.3 [7.1 - 8.5]	$p > 0.05$	$p > 0.05$
	Pb	8.1 [7.5 - 8.4]	8.0 [7.6 - 8.2]	$p > 0.05$	$p > 0.05$
	Zn	8.2 [7.7 - 8.4]	8.1 [7.6 - 8.3]	$p > 0.05$	$p > 0.05$
Cd	Ag	69 [58 - 80]	72 [58 - 85]	7.7 [7.2 - 7.9]	7.6 [6.9 - 7.9]
	Cu	54 [43 - 65]	51 [43 - 59]	8.2 [7.4 - 8.5]	8.1 [7.8 - 8.3]
	Ni	82 [65 - 98]	86 [70 - 102]	$p > 0.05$	$p > 0.05$
	Pb	59 [52 - 66]	56 [45 - 67]	$p > 0.05$	$p > 0.05$
	Zn	48 [42 - 54]	52 [42 - 62]	$p > 0.05$	$p > 0.05$
Cu (see note)	Ag	4.6 [3.4 - 5.7]	3.6 [2.6 - 4.7]	7.7 [6.7 - 8.0]	7.8 [7.1 - 8.1]
	Cd	5.3 [3.0 - 7.7]	3.3 [1.9 - 4.7]	$p > 0.05$	$p > 0.05$
	Ni	2.1 [1.4 - 2.8]	1.4 [1.0 - 1.8]	$p > 0.05$	$p > 0.05$
	Pb	1.9 [0.8 - 3.1]	2.1 [0.9 - 3.2]	$p > 0.05$	$p > 0.05$
	Zn	2.8 [1.7 - 3.8]	2.5 [1.7 - 3.3]	$p > 0.05$	$p > 0.05$
Ni	Ag	9.6 [7.5 - 12]	9.6 [7.9 - 11]	$p > 0.05$	$p > 0.05$
	Cd	5.1 [3.8 - 6.5]	6.2 [4.2 - 8.2]	$p > 0.05$	$p > 0.05$
	Cu	6.2 [4.2 - 8.2]	8.1 [6.9 - 9.3]	$p > 0.05$	$p > 0.05$
	Pb	5.7 [4.0 - 7.3]	6.1 [4.7 - 7.4]	$p > 0.05$	$p > 0.05$
	Zn	4.5 [3.7 - 5.2]	5.7 [4.3 - 7.0]	$p > 0.05$	$p > 0.05$
Pb	Ag	4.9 [3.2 - 6.5] *	7.4 [5.6 - 9.3] *	$p > 0.05$	7.3 [6.4 - 7.6]
	Cd	10 [7.5 - 13]	7.6 [5.0 - 10]	$p > 0.05$	$p > 0.05$
	Cu	7.3 [5.4 - 9.1]	8.1 [4.9 - 11]	$p > 0.05$	$p > 0.05$
	Ni	9.1 [5.8 - 12]	8.2 [6.0 - 10]	$p > 0.05$	$p > 0.05$
	Zn	8.5 [3.9 - 13]	14 [9.2 - 19]	$p > 0.05$	$p > 0.05$
Zn	Ag	35 [30 - 40]	37 [27 - 446]	7.2 [6.6 - 7.4]	7.4 [5.8 - 7.7]
	Cd	42 [11 - 73]	50 [33 - 67]	$p > 0.05$	$p > 0.05$
	Cu	42 [34 - 51]	40 [32 - 48]	8.1 [7.7 - 8.3]	8.2 [7.9 - 8.4]
	Ni	41 [35 - 47] *	29 [24 - 33] *	$p > 0.05$	$p > 0.05$
	Pb	39 [30 - 48]	29 [22 - 37]	$p > 0.05$	$p > 0.05$

Note: The % Cu^{2+} considerably varied with Pb, Ni and Zn (as described in Table SI.2) and these regression analyses were performed on mean (Cu^{2+}) values.

In the mixture exposures, the WHAM VII calculations suggest that the proportion of Ni^{2+} in solution was negligibly affected by the presence of a second metal (Table SI.2). Nickel uptake in *L. stagnalis* was not affected by the presence of any other metal in solution. (Fig. 5, Table 2).

3.5. Lead uptake

In the exposures with Pb only, Pb was equally accumulated by the different snail biological compartments analyzed in this study (Fig. 1E). In the Pb-alone uptake tests, the proportion of free Pb^{2+} in solution varied slightly from 5.6 to 7.3% (based on activity) within the range of the total dissolved Pb concentration (Table SI.1). As for Cu, this increase was attributed to a gradual occupancy of the finite number of DOM binding sites with the increase of aqueous Pb (with a decrease of Pb-DOM from 53 to 38%). Lead uptake fluxes in the soft tissues of *L. stagnalis* showed a Michaelis-Menten type of relationship with $\{Pb^{2+}\}$ (Fig. 6A). The fitted J_{max} was $7.7 nmol \cdot g^{-1} \cdot h^{-1}$ and the apparent K_{Pb} was $10^{8.3} M^{-1}$ (Table 1). When the analysis was based on total dissolved concentration, K_{Pb} considerably decreased to $10^{6.6} M^{-1}$ (Table SI.3).

In the mixture exposures, the WHAM VII calculations suggest that the presence of a second metal negligibly affected the proportion of Pb^{2+} in solution (by <1.3-fold) (Table SI.2). Nickel, Pb and Zn had no effect on Pb uptake in *L. stagnalis*. A small but significant 30% inhibitory effect occurred within the tested/chronic Ag concentration range, but only at the highest Pb concentration tested (Fig. 6B). For this effect, the conditional affinity constant of Ag for the Pb transporter was of $10^{7.3} M^{-1}$ ($p = 0.033$) (Table 2). In addition, a small but significant increase of $J_{max, Pb}$ value (by 1.5-fold, $p = 0.026$) occurred (Table 2), suggesting an un-competitive type of effect.

3.6. Zinc uptake

In the exposures with Zn only, Zn was around 5-times more concentrated in the digestive tract than in the rest of soft tissues analyzed (Fig. 1F). According to the WHAM VII calculations for the Zn-alone uptake tests, Zn^{2+} was the most important of the dissolved species (53%, based on activity). Other significant chemical species were hydroxo, carbonato-, sulfato- and DOM-complexes, in comparable proportions. Zinc uptake fluxes in the soft tissues of *L. stagnalis* showed a Michaelis-Menten type of relationship with $\{Zn^{2+}\}$ (Fig. 7A). The fitted J_{max} was $32 nmol \cdot g^{-1} \cdot h^{-1}$ and the fitted apparent K_{Zn} was $10^{5.1} M^{-1}$ (Table 1). When the analysis was based on total dissolved concentration, the K_{Zn} value decreased slightly to $10^{4.9} M^{-1}$ (Table SI.3).

In the mixture exposures, the WHAM VII calculations suggest that the proportion of Zn^{2+} in solution was negligibly affected by the presence of a second metal (Table SI.2). Cadmium and Pb had no effect on Zn_{int} values (Fig. 7C, F and Table 2). Silver and Cu both inhibited Zn uptake fluxes in a manner that could be captured by the BLM (Fig. 7B, D and Table 2). Regressions with Eq. (3) provided conditional affinity constants of Ag and Cu for the Zn transporter of around $10^{7.4}$ and $10^{8.2} M^{-1}$, respectively (with no apparent effect of these second metals on $J_{max, Zn}$). Overall, the Ag effects on Zn_{int} were a 60% decrease within the tested Ag concentration ranges (0–80 nM Ag^+) and a 30% decrease within the Ag chronic concentration ranges (0–30 nM Ag^+). The Cu effects on Zn_{int} were a 50% decrease within the tested Cu concentration ranges (0–12 nM Cu^{2+}) and a 40% decrease within the Cu chronic concentration ranges (0–6 nM Cu^{2+}). Finally, in the presence of Ni, $J_{max, Zn}$ was slightly but significantly decreased (by 1.4-fold, $p = 0.001$) at the highest compared to the lowest Zn concentration tested (Fig. 7E and Table 2).

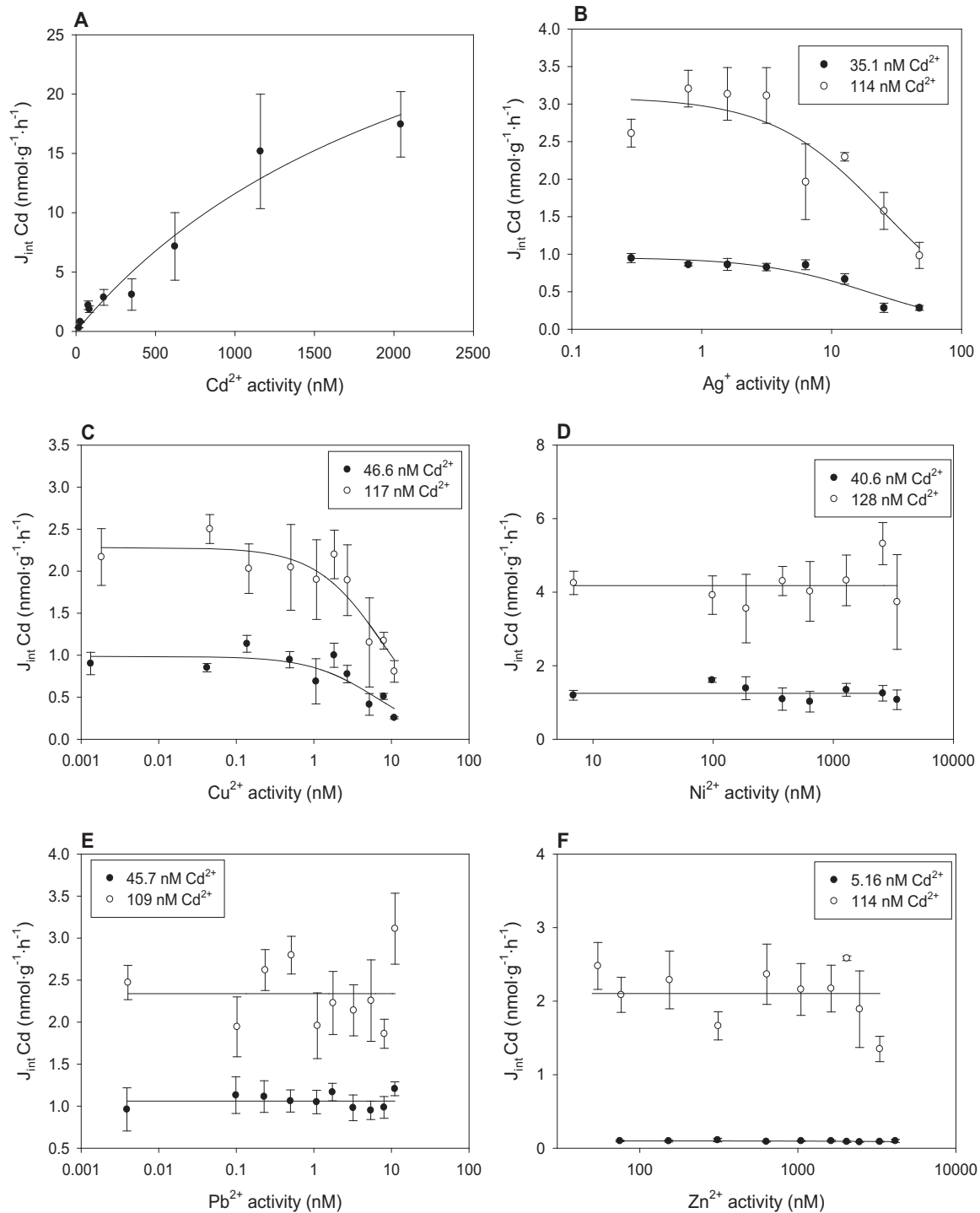


Fig. 3. Internalization flux of Cd in the soft tissues of *L. stagnalis* exposed for 2 h, as a function of the calculated aqueous activity of A) Cd^{2+} , B) Ag^+ , C) Cu^{2+} , D) Ni^{2+} , E) Pb^{2+} and F) Zn^{2+} . Values are mean \pm SE ($n = 3$). Data in panel A were obtained from a single-metal uptake test and are fitted with Eq. (2) (plain line). Data in panels B, C, D, E and F were obtained from binary mixture tests at two Cd^{2+} concentrations (white and black circles) and were fitted with Eq. (3) (plain lines: regression lines, with K_{M2} set to 0 when found to be non-significant ($p > 0.05$)).

4. Discussion

4.1. Single-metal uptake

4.1.1. Metal tissue distribution

The uptake of both trace metals and major ions generally occurs *via* the gills in aquatic organisms. However, as a pulmonate snail, *L. stagnalis* does not have gills, so much of the ion uptake in this species is thought to occur across the skin, over the whole exposed epithelial surface (Boer and Witteveen, 1980; Schlichter, 1982). In the present study, the short-term

metal distribution patterns observed in the soft tissues agreed with this assumption. Indeed, differential soft tissue accumulation was only observed for Ag, for which accumulation seemed very slightly higher in the foot and the mantle. With regards to accumulation in the digestive tract, different patterns emerged. A slightly lower to similar concentration was observed in the digestive tract compared to soft tissue for Ag, Cu, Ni and Pb. On the other hand, a higher concentration was observed in the digestive tract for Cd (3-fold) and Zn (6-fold). Since the snail digestive system is not directly in contact with the ambient water, a low metal accumulation in the digestive tract could be *a priori* expected in our

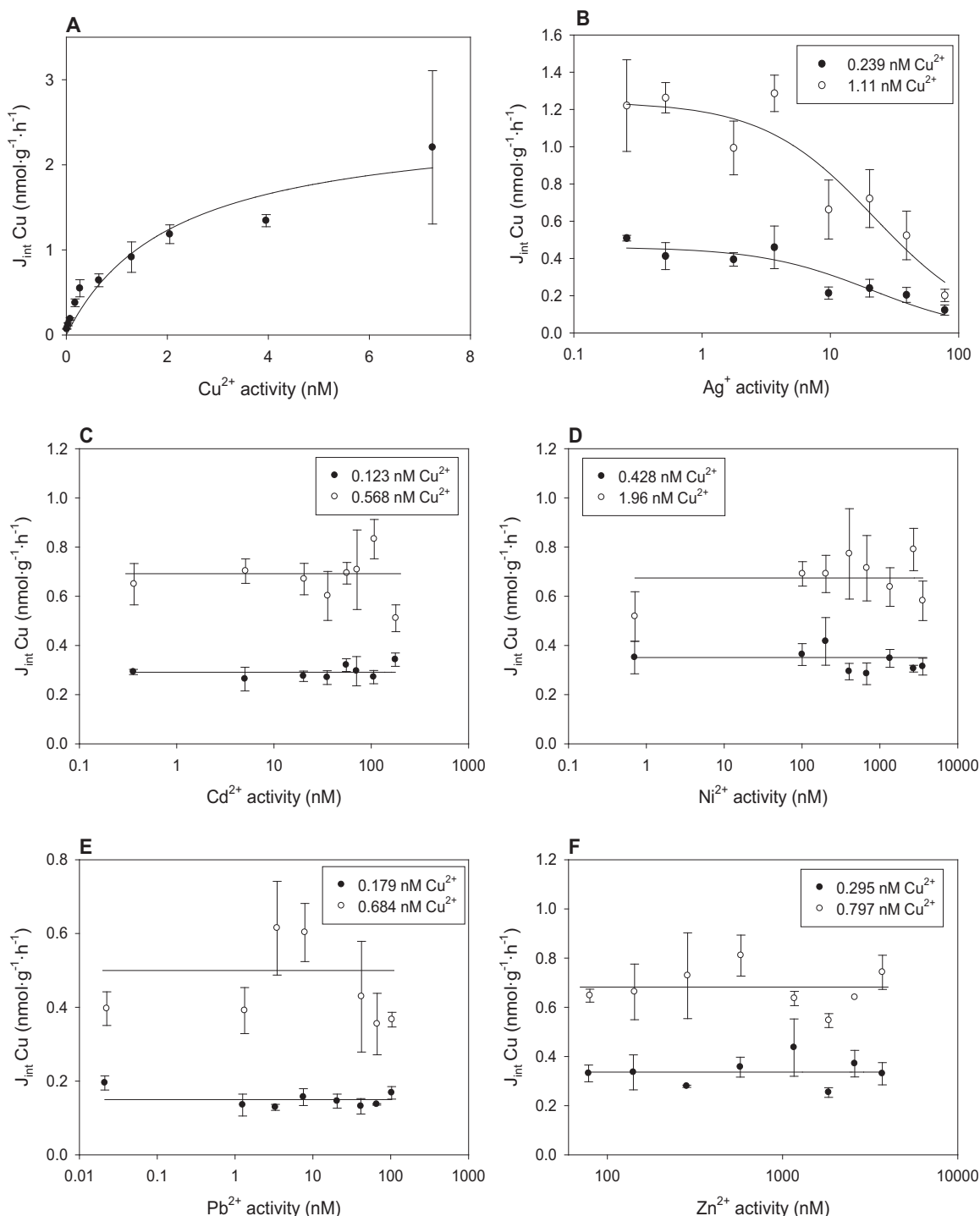


Fig. 4. Internalization flux of Cu in the soft tissues of *L. stagnalis* exposed for 2 h, as a function of the calculated aqueous activity of A) Cu^{2+} , B) Ag^+ , C) Cd^{2+} , D) Ni^{2+} , E) Pb^{2+} and F) Zn^{2+} . Values are mean \pm SE ($n = 3$). Data in panel A were obtained from a single-metal uptake test and are fitted with Eq. (2) (plain line). Data in panels B, C, D, E and F were obtained from binary mixture tests at two Cu^{2+} concentrations (white and black circles) and were fitted with Eq. (3) (plain lines; regression lines, with K_{M2} set to 0 when found to be non-significant ($p > 0.05$)). Note that while mean $[\text{Cu}^{2+}]$ are given in each panel (and were used for regression analysis), the % Cu^{2+} considerably varied with Pb, Ni and Zn (as described in Table S1.2).

short-term uptake tests. However, oral water ingestion is known to occur in *L. stagnalis* (De With, 1996). Hence, the metal concentrations observed in the digestive tract could reflect the ambient metal concentration. A similar water ingestion rate across the different uptake tests, associated with differential levels of metal uptake through the skin may partially explain the different proportion of digestive tract vs. soft tissues concentration across metals. Note also that, similarly to Cd and Zn, Pb was quite elevated in the digestive tract (although not significantly higher than in the soft tissues). Yet, these three metals are considered to be Ca-

analogues (Hogstrand et al., 1996; Wood, 2001; Rogers et al., 2003; Muysen et al., 2006). Hence, this pattern may indicate some preferential Ca uptake pathways in the digestive tract of *L. stagnalis*. Based on these results, metal uptake was measured in the whole soft tissues without the digestive tracts in the subsequent experiments.

4.1.2. Kinetics of metal uptake

For each metal M, the relationship between J_{int} and $\{\text{M}^{2+}\}$ was well captured by Eq. (2) of the BLM, although Ag did not show a saturation

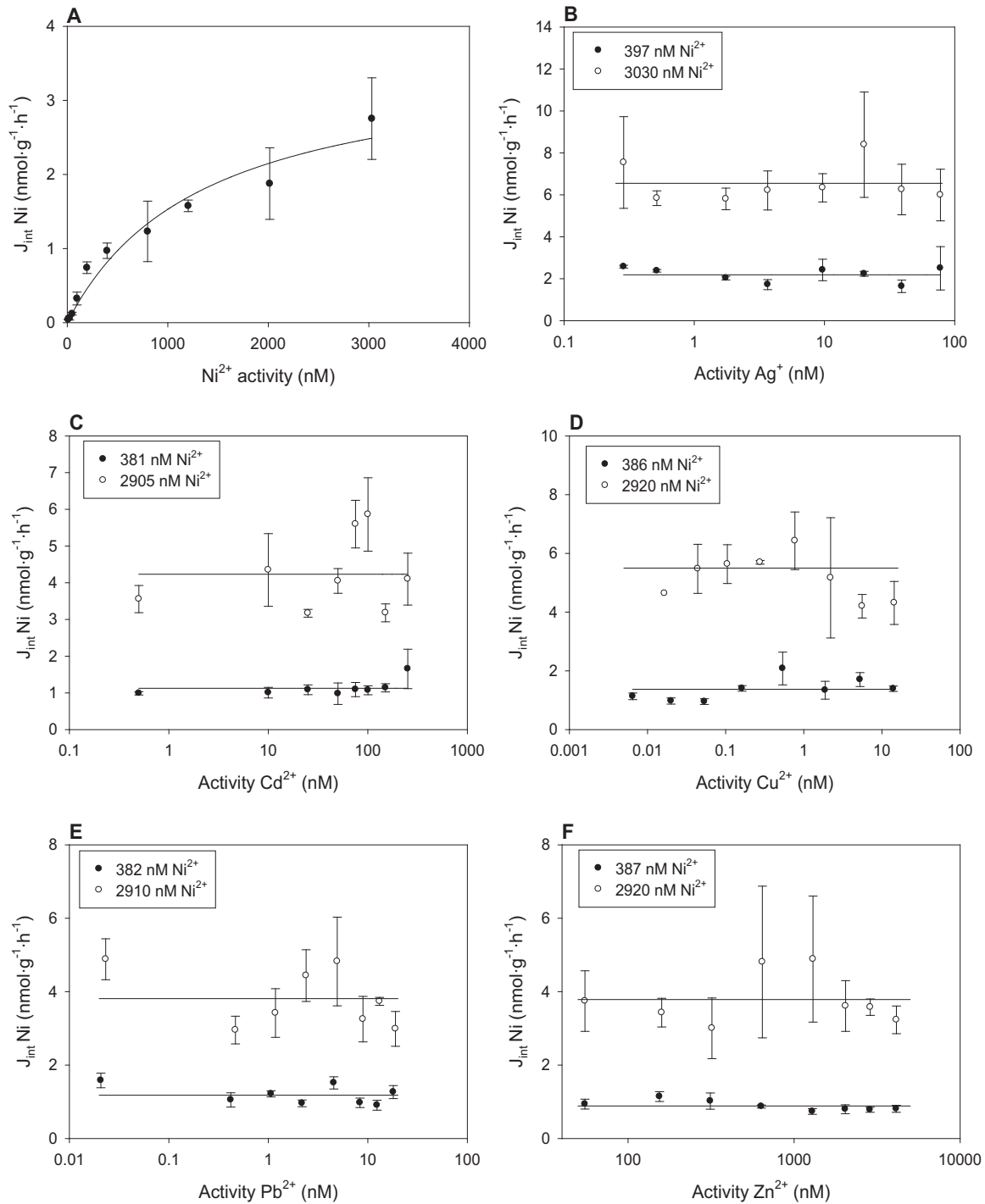


Fig. 5. Internalization flux of Ni in the soft tissues of *L. stagnalis* exposed for 2 h, as a function of the calculated aqueous activity of A) Ni^{2+} , B) Ag^+ , C) Cd^{2+} , D) Cu^{2+} , E) Pb^{2+} and F) Zn^{2+} . Values are mean \pm SE ($n = 3$). Data in panel A were obtained from a single-metal uptake test and are fitted with Eq. (2) (plain line). Data in panels B, C, D, E and F were obtained from binary mixture tests at two Ni^{2+} concentrations (white and black circles) and were fitted with Eq. (3) (plain lines: regression lines, with K_{M2} set to 0 when found to be non-significant ($p > 0.05$)).

profile over the range of $\{\text{Ag}^+\}$ tested. The metal transport capacity, quantified by the obtained J_{max} values, decreased by 16-fold in the order $\text{Cd} \sim \text{Zn} > \text{Pb} > \text{Cu} \sim \text{Ni}$, while the J_{max} value of Ag was higher than that of Cu and Ni. The metal-transporter apparent affinities, quantified by the obtained affinity constants K_M , were within the range of values generally reported for metal uptake to other aquatic organisms, such as the extensively studied rainbow trout (see e.g. $K_m (=1 / K_M)$ Michaelis-Menten values reported by Brix et al., 2016, 2017). Note that these K_M values are conditional to the water ionic composition, as they may include the competing effects of ions such as Ca^{2+} , Mg^{2+} ,

H^+ or Na^+ , which would decrease their true values. The observed K_M values increased by 3400-fold in the order $\text{Zn} < \text{Ni} < \text{Pb} < \text{Cu}$, while K_{Ag} was higher than Cd, Ni and Zn K_M values. For Cd, the large uncertainty around its K_M estimate did not lead to any significant difference with the other metals. Interestingly, the observed order in K_M values was in agreement with the order in the chronic sensitivity of juvenile *L. stagnalis* to these six metals observed in a previous study (Crémazy et al., 2018). In this latter work, we estimated the free ion activities at 50% effect from 14-d growth tests with juvenile snails. These $\text{EC}_{50_{Mz+}}$ values, inversely proportional to snail sensitivity, increased in the

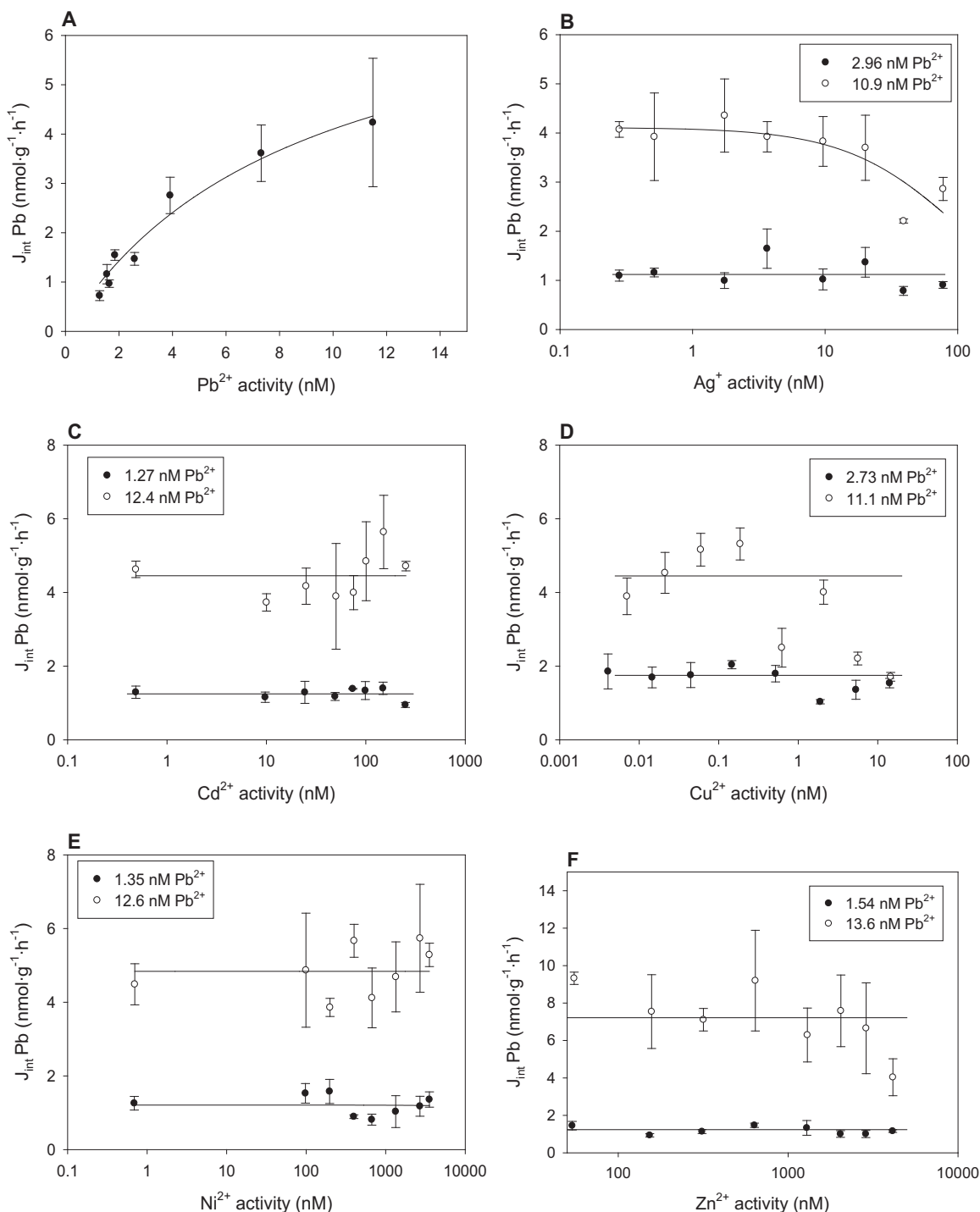


Fig. 6. Internalization flux of Pb in the soft tissues of *L. stagnalis* exposed for 3 h, as a function of the calculated aqueous activity of A) Pb^{2+} , B) Ag^+ , C) Cd^{2+} , D) Cu^{2+} , E) Ni^{2+} and F) Zn^{2+} . Values are mean \pm SE ($n = 3$). Data in panel A were obtained from a single-metal uptake test and are fitted with Eq. (2) (plain line). Data in panels B, C, D, E and F were obtained from binary mixture tests at two Pb^{2+} concentrations (white and black circles) and were fitted with Eq. (3) (plain lines: regression lines, with K_{M2} set to 0 when found to be non-significant ($p > 0.05$)).

following order: $\text{Cu} < \text{Pb} < \text{Ag} < \text{Cd} < \text{Ni} < \text{Zn}$. The resulting positive relationship between metal binding constant K_M and metal chronic sensitivity to *L. stagnalis* is similar to the relationship observed between K_M and acute sensitivity in rainbow trout (Niyogi and Wood, 2004), although the ordering of metals differs somewhat. As in rainbow trout, it suggests a potential link between short-term metal uptake and, in this case, long-term metal toxicity in this organism. Mechanisms of chronic toxicity are generally much more complex than acute toxicity, as many time-dependent physiological processes may come into play, including uptake, translocation, metabolism and depuration. Yet, as a

first step of metal-organism interaction, short-term metal uptake rates could be an indicator of long-term tissue accumulation, which in term may indicate chronic toxicity (Adams et al., 2011). In line with this assumption, past studies on *L. stagnalis* showed that chronic sensitivity to metals may be related to poor regulation of metal body burden, i.e. to high metal accumulation (Amiard and Amiard-Triquet, 1979; Pyatt et al., 1997, 2003; Croteau and Luoma, 2009; Niyogi et al., 2014). In agreement with these studies, we have observed significant tissue bioaccumulation of all six metals in the 14-d toxicity tests conducted with juvenile *L. stagnalis* (Fig. S1.2 in the Supporting information).

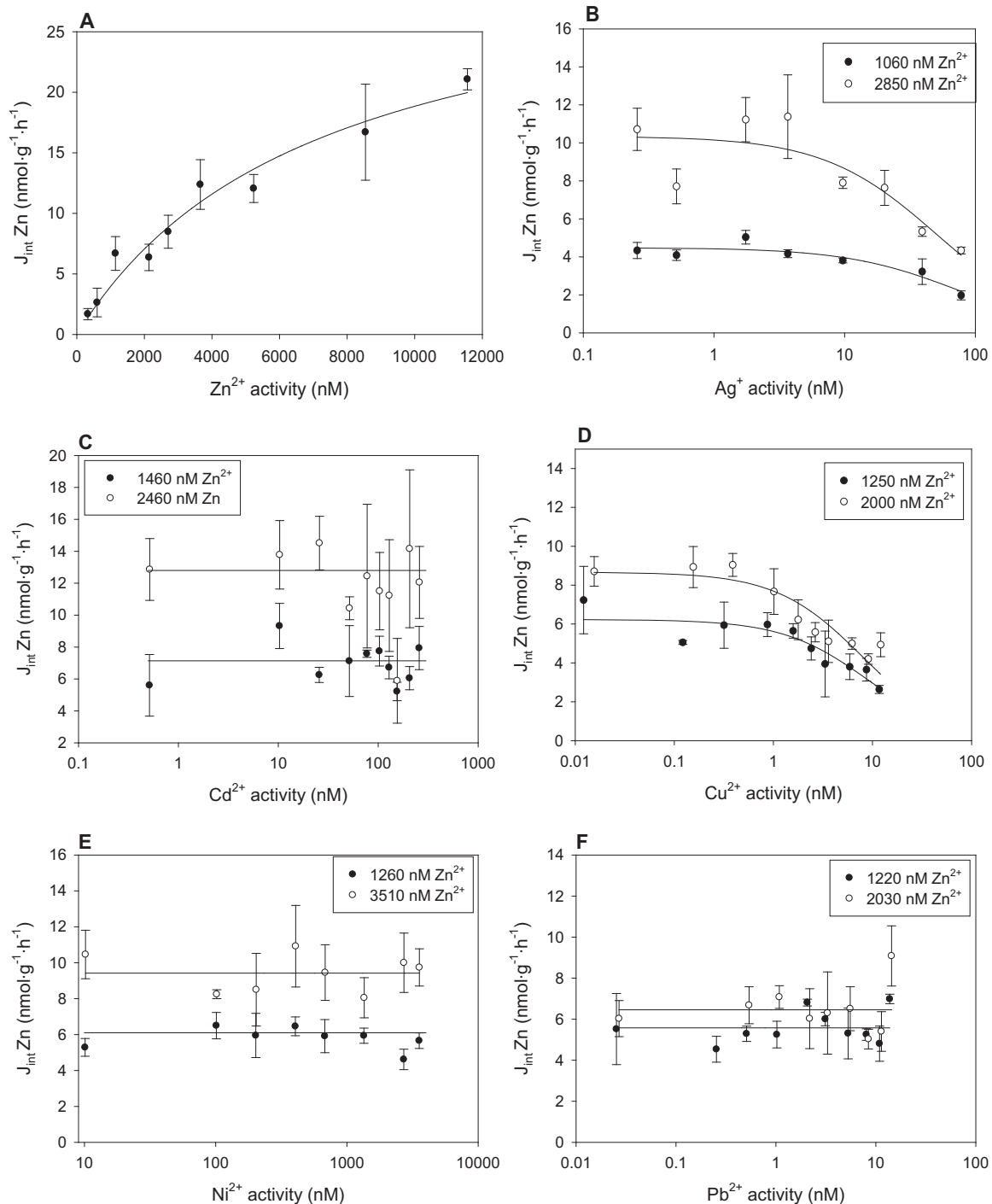


Fig. 7. Internalization flux of Zn in the soft tissues of *L. stagnalis* exposed for 2 h, as a function of the calculated aqueous activity of A) Zn^{2+} , B) Ag^+ , C) Cd^{2+} , D) Cu^{2+} , E) Ni^{2+} and F) Pb^{2+} . Values are mean \pm SE ($n = 3$). Data in panel A were obtained from a single-metal uptake test and are fitted with Eq. (2) (plain line). Data in panels B, C, D, E and F were obtained from binary mixture tests at two Zn^{2+} concentrations (white and black circles) and were fitted with Eq. (3) (plain lines: regression lines, with K_{M2} set to 0 when found to be non-significant ($p > 0.05$)).

4.2. Multi-metals interactions

Two important types of multi-metal interactions were characterized in the present study: (i) geochemical interactions in the exposure water and (ii) interactions at the site of biological uptake. The first type of interaction was predicted by thermodynamic calculations with WHAM VII. According to these calculations, limited DOM binding sites for Cu, a metal with a chemical speciation that is strongly dominated by DOM complexes, made Cu speciation particularly sensitive to the presence of a second metal in solution. Indeed, because of competition for complexation to the same binding sites on the DOM, free Cu^{2+} ion activity

increased in the presence of Ni (up to 1.8-fold), Pb (up to 3.4-fold) and Zn in solution (up to 9.5-fold). According to the BLM, an increase in free metal ion activity should lead to a corresponding increase in metal uptake, provided that the transport system is not already saturated, and that the concentration of competing ions is kept constant (cf. Eqs. (2) and (3)). Hence, this type of multi-metal interaction has the capacity to explain more-than-additive multi-metal interactions for uptake. Yet, in the present study, there was no effect of Ni, Pb or Zn on Cu uptake (cf. Fig. 2D, E, F). We identified three possible explanations for these observations. First, competition of Ni^{2+} , Pb^{2+} and Zn^{2+} with Cu^{2+} at the membrane transporter for Cu could theoretically

cancel out the positive effect of the increased $\{Cu^{2+}\}$ on Cu uptake caused by competition at DOM sites. However, it seems rather unlikely that a perfect counter-balance between these two opposing effects would fortuitously be obtained for these three binary metal combinations in the present study. A second explanation could be that Cu uptake by *L. stagnalis* constitutes an exception to the BLM and therefore does not follow its predictions. Deviation from the model occurs if one or more of its underlying assumptions are not fulfilled (e.g. metal complexes such as Cu-DOM complexes should not be bioavailable). Previous studies have shown that the BLM framework was rather successful at predicting Ni and Zn chronic toxicity to *L. stagnalis* in natural waters with different chemistries (including broad ranges of DOC concentrations) (De Schampelaere and Janssen, 2010; Schlegel et al., 2010). Yet, the BLM remains to be specifically tested for Cu uptake in *L. stagnalis*. Finally, a third explanation could lie in the inherent uncertainties surrounding chemical speciation calculations from thermodynamic software such as WHAM. Indeed, different sources of uncertainties may lead to relatively large errors in metal speciation predictions: uncertainties on the input water chemistry, on the assumptions made on metal-DOM binding properties and on the thermodynamic constants used in the software (Unsworth et al., 2006; Tipping et al., 2011). In our study, these errors may have led to over-estimating the competition between Cu^{2+} and Ni^{2+} , Pb^{2+} and Zn^{2+} for DOM binding sites.

Out of the 15 binary mixtures tested in this study, multi-metal effects on biological uptake were observed for 7 of them. Virtually all the effects were caused by either Ag or Cu, and were inhibitory in nature. These effects at most represented a 50% (i.e., 2-fold) reduction in metal uptake. In the present study, this second type of multi-metal interaction was analyzed using the BLM conceptual framework. In theory, for a binary metal mixture, the BLM can model strictly additive uptake with a two-site model (with one independent uptake site for each metal) and less-than-additive uptake (i.e., antagonistic interactions) with a one-site model (with metals competing for binding to this same transport site). On the other hand, without geochemical interactions leading to increased free ion activities (as described above), more-than-additive uptake cannot be explained by the BLM and would indicate a deviation from its underlying premises (e.g. the physiology of the organism should remain unchanged over the time of exposure). In the present study, the BLM could partially to fully explain multi-metal interactions observed for 5 mixtures (Ag/Cu, Ag/Cd, Cd/Cu, Zn/Ag, Zn/Cu), but could not explain the (very small) effects observed for 2 mixtures (Ag/Pb and Ni/Zn). Silver and Cu both affected each others' uptake, but in different ways. The BLM predicted a competitive inhibition from Ag (M_2) on Cu (M_1) uptake, with a K_{M_2} about one order of magnitude lower than the conditional K_{M_1} . Note however that contrary to K_{M_1} , K_{M_2} is not conditional on the ionic composition of the exposure medium, which limits the direct comparison between the two parameters. Copper, however, seemed to affect Ag uptake in a more complex manner which could not be captured by the BLM, as a slight enhancement followed by an inhibition of Ag uptake was observed within the Cu concentration range tested. This type of hormesis effect on metal uptake from a secondary metal has been reported previously (Chen et al., 2010). In the present study, it may be indicative of a physiological effect of Cu on Ag transporter capacity that would modulate $J_{max,Ag}$ (e.g., a change in the density of Ag transporters or in their conformation). Stimulatory effects on uptake have also been observed by Niyogi et al. (2015) in rainbow trout exposed to a Ag/Cu mixture. However, in this latter study, it was Cu uptake which appeared to be stimulated by Ag. Further investigations are needed to fully understand the apparent complexity of the Ag/Cu interactions at the water-organism interface. In addition to the effect of Cu on Ag uptake, non-competitive or uncompetitive effects that could not be explained by the BLM were also observed for Ag/Pb and Ni/Zn mixtures in our study. Indeed, Ag slightly inhibited (30% decrease) Pb uptake, but only at the highest Pb concentration tested, where a small increase of J_{max} ,

Pb value (by 1.5-fold) also occurred. In addition, in the presence of Ni, $J_{max,Zn}$ was slightly different between the two Zn concentrations tested (by 1.4-fold). These small changes in J_{max} suggest physiological effects occurring on metal transport capacity. Further work is needed to fully characterize these types of effects and evaluate their environmental relevance. Finally, Ag and Cu both inhibited Cd and Zn uptake (but not vice-versa), in a competitive way that was captured by the BLM. These latter interactions were less expected than interactions between Ag and Cu. Indeed, physiological studies on metal toxicity to aquatic organisms have led to a traditional classification of trace metals into two categories within which metal interactions are considered more likely to occur: (i) Na-antagonists, comprising Ag and Cu (Grosell et al., 2002) and (ii) Ca-antagonists, comprising Cd, Pb and Zn (Hogstrand et al., 1996; Wood, 2001; Rogers et al., 2003; Muysen et al., 2006). However, this classification originates from acute toxicity studies that were conducted with fish at higher metal concentrations, and may hence not apply in the present chronic study with *L. stagnalis*. Indeed, observations suggest that disruption of Ca homeostasis is associated with chronic metal toxicity to *L. stagnalis*. Yet, *L. stagnalis* is very sensitive to Cu (Brix et al., 2011; Crémazy et al., 2018), but relatively insensitive to Zn (De Schampelaere and Janssen, 2010). Furthermore, even previous metal mixture studies with fish have reported interactions that were not following predictions based on the Ca-/Na-antagonist classification (Niyogi et al., 2015; Brix et al., 2016; Brix et al., 2017). For example, as in the present study, Cu has previously been shown to inhibit Cd binding to fish gills (Pelgrom et al., 1995; Komjarova and Blust, 2009; Niyogi et al., 2015).

4.3. Environmental relevance

As for the observed multi-metals interactive effects on metal chronic toxicity to *L. stagnalis* (Crémazy et al., 2018), the amplitude of the interactive effects on short-term uptake observed in the present study were generally very small in the chronic concentration ranges. Hence, a first important conclusion from this work is that the bias generated from modeling metal uptake without accounting for multi-metal joint effects will remain relatively low. Second, the BLM could capture most of the important multi-metal effects observed on metal uptake in *L. stagnalis*, while a few non-competitive or uncompetitive effects were also observed. Hence, from the uptake dataset obtained in the present study, a metal mixture BLM for uptake (mBLM) could be developed to explain the uptake patterns of most binary metal mixtures in *L. stagnalis*. However, it should be noted that while the present uptake study offers some valuable insights into possible multi-metal interactions on uptake mechanisms in *L. stagnalis*, important areas of uncertainties remain. Notably, it should be emphasized that an observed inhibition of M_1 uptake by M_2 does not necessarily mean that M_2 uses M_1 transporters. Indeed, M_2 could bind to M_1 uptake sites, effectively blocking M_1 internalization, without being subsequently taken up itself. Certainly, a given metal can bind to a variety of "inert" and "active" sites at biological membranes (Slaveykova and Wilkinson, 2002). Furthermore, a metal can use different membrane transporters with different affinities and capacities in a same species (Lavoie et al., 2012). Unfortunately, the identity and number of transporters used by Ag, Cd, Cu, Ni, Pb and Zn in *L. stagnalis* remain virtually unknown. Thus, additional studies would have to be undertaken to obtain full unequivocal characterization of metal mixture uptake in *L. stagnalis*, although the present study allowed the formulation of useful assumptions on the nature of multi-metal interactions for future modeling work.

While the links between short-term metal uptake and long-term metal toxicity remain elusive in *L. stagnalis*, a few parallels were observed between the uptake data from this study and the toxicity data from Crémazy et al. (2018). Indeed, there was a good agreement between the short-term metal transport affinity K_M and the chronic EC values previously obtained. Furthermore, the multi-metal interactions observed on both short-term uptake and long-term toxicity were

generally of low amplitude. However, while some of the antagonisms previously observed in metal mixture chronic toxicity could be potentially explained by competition for short-term metal uptake (e.g. for Cu/Zn and Ag/Zn mixtures), other observations on metal mixture toxicity were not supported by the present short-term data. For example, the more-than-additive chronic toxicity observed for the Cd/Ni mixture and the less-than-additive chronic toxicity observed for the Cd/Zn mixture were not supported by the uptake data, as no interaction for uptake was observed between these metals. These observations probably suggest that multi-metals interactions exist at other biological levels affecting chronic toxicity (e.g. detoxification), and that the site of uptake and the site of action are not necessarily the same. Thus, a mBLM derived from the current uptake dataset would not suffice to model multi-metals chronic toxicity to *L. stagnalis*, but would rather constitute a first mathematical component of a more complex metal mixture toxicity model (e.g. a Toxicokinetic-Toxicodynamic model).

Acknowledgements

The authors acknowledge TRIUMF, and more precisely Dr. Stefan Zeisler and Hua Zhang, for producing the Cu-64 that was used in the present study. This research was supported by funding from the Copper Development Association (CDA), the International Copper Association (ICA), the International Zinc Association (IZA), the Nickel Producers Environmental Research Association (NiPERA), Rio Tinto, and an NSERC CRD grant to CMW and Dr. Soumya Niyogi. KVB was supported by an NSF Postdoctoral Fellowship (DBI-1306452) and CMW was supported by the Canada Research Chairs Program.

Appendix A. Supplementary data

Supplementary data to this article can be found online at <https://doi.org/10.1016/j.scitotenv.2018.07.455>.

References

- Adams, W.J., Blust, R., Borgmann, U., Brix, K.V., Deforest, D.K., Green, A.S., Meyer, J., McGeer, J.C., Paquin, P., Rainbow, P.S., Wood, C.M., 2011. Utility of tissue residues for predicting effects of metals on aquatic organisms. *Integr. Environ. Assess. Manag.* 7, 77–98.
- Amiard, J.C., Amiard-Triquet, C., 1979. Distribution of cobalt 60 in a mollusc, a crustacean and a freshwater teleost: variation as a function of the source of pollution and during elimination. *Environ. Pollut.* 20, 199–213.
- Ardestani, M.M., Van Straalen, N.M., Van Gestel, C.A.M., 2014. The relationship between metal toxicity and biotic ligand binding affinities in aquatic and soil organisms: a review. *Environ. Pollut.* 195, 133–147.
- Backhaus, T., Faust, M., 2012. Predictive environmental risk assessment of chemical mixtures: a conceptual framework. *Environ. Sci. Technol.* 46, 2564–2573.
- Balistreri, L.S., Mebane, C.A., 2014. Predicting the toxicity of metal mixtures. *Sci. Total Environ.* 466, 788–799.
- Balistreri, L.S., Mebane, C.A., Schmidt, T.S., Keller, W.B., 2015. Expanding metal mixture toxicity models to natural stream and lake invertebrate communities. *Environ. Toxicol. Chem.* 2015 (34), 761–776.
- Boer, H.H., Witteveen, J., 1980. Ultrastructural localization of carbonic anhydrase in tissues involved in shell formation and ionic regulation in the pond snail *Lymnaea stagnalis*. *Cell Tissue Res.* 209, 383–390.
- Brix, K.V., Esbaugh, A.J., Grosell, M., 2011. The toxicity and physiological effects of copper on the freshwater pulmonate snail, *Lymnaea stagnalis*. *Comp. Biochem. Physiol. C: Toxicol. Pharmacol.* 154, 261–267.
- Brix, K.V., Esbaugh, A.J., Munley, K.M., Grosell, M., 2012. Investigations into the mechanism of lead toxicity to the freshwater pulmonate snail, *Lymnaea stagnalis*. *Aquat. Toxicol.* 106, 147–156.
- Brix, K.V., Tellis, M.S., Crémazy, A., Wood, C.M., 2016. Characterization of the effects of binary metal mixtures on short-term uptake of Ag, Cu, and Ni by rainbow trout (*Oncorhynchus mykiss*). *Aquat. Toxicol.* 180, 236–246.
- Brix, K.V., Tellis, M.S., Crémazy, A., Wood, C.M., 2017. Characterization of the effects of binary metal mixtures on short-term uptake of Cd, Pb, and Zn by rainbow trout (*Oncorhynchus mykiss*). *Aquat. Toxicol.* 193, 217–227.
- Bryan, S.E., Tipping, E., Hamilton-Taylor, J., 2002. Comparison of measured and modelled copper binding by natural organic matter in freshwaters. *Comp. Biochem. Physiol. C: Toxicol. Pharmacol.* 133, 37–49.
- Buffle, J., 1988. *Complexation Reactions in Aquatic Systems: An Analytical Approach*. John Wiley.
- Chen, Z., Zhu, L., Wilkinson, K.J., 2010. Validation of the biotic ligand model in metal mixtures: bioaccumulation of lead and copper. *Environ. Sci. Technol.* 44, 3580–3586.
- Crémazy, A., Brix, K.V., Wood, C.M., 2018. Chronic toxicity of binary mixtures of six metals (Ag, Cu, Cd, Pb, Ni and Zn) to the great pond snail *Lymnaea stagnalis*. *Environ. Sci. Technol.* 52, 5979–5988.
- Croteau, M.N., Luoma, S.N., 2009. Predicting dietborne metal toxicity from metal influxes. *Environ. Sci. Technol.* 43, 4915–4921.
- De Schampelaere, K.A.C., Janssen, C.R., 2010. Cross-phylum extrapolation of the *Daphnia magna* chronic biotic ligand model for zinc to the snail *Lymnaea stagnalis* and the rotifer *Brachionus calyciflorus*. *Sci. Total Environ.* 408, 5414–5422.
- De Schampelaere, K.A.C., Koene, J.M., Heijerick, D.G., Janssen, C.R., 2008. Reduction of growth and haemolymph Ca levels in the freshwater snail *Lymnaea stagnalis* chronically exposed to cobalt. *Ecotoxicol. Environ. Saf.* 71, 65–70.
- De With, N.D., 1996. Oral water ingestion in the pulmonate freshwater snail, *Lymnaea stagnalis*. *J. Comp. Physiol. B.* 166, 337–343.
- Di Toro, D.M., Allen, H.E., Bergman, H.L., Meyer, J.S., Paquin, P.R., Santore, R.C., 2001. Biotic ligand model of the acute toxicity of metals. 1. Technical basis. *Environ. Toxicol. Chem.* 20, 2383–2396.
- Esbaugh, A.J., Brix, K.V., Mager, E.M., De Schampelaere, K.A.C., Grosell, M., 2012. Multi-linear regression analysis, preliminary biotic ligand modeling, and cross species comparison of the effects of water chemistry on chronic lead toxicity in invertebrates. *Comp. Biochem. Physiol. C: Toxicol. Pharmacol.* 155, 423–431.
- Farley, K.J., Meyer, J.S., 2015. Metal mixture modeling evaluation project: 3. Lessons learned and steps forward. *Environ. Toxicol. Chem.* 34, 821–832.
- Grosell, M., Brix, K.V., 2009. High net calcium uptake explains the hypersensitivity of the freshwater pulmonate snail, *Lymnaea stagnalis*, to chronic lead exposure. *Aquat. Toxicol.* 91, 302–311.
- Grosell, M., Nielsen, C., Bianchini, A., 2002. Sodium turnover rate determines sensitivity to acute copper and silver exposure in freshwater animals. *Comp. Biochem. Physiol. C: Toxicol. Pharmacol.* 133, 287–303.
- Hassler, C.S., Slaveykova, V.I., Wilkinson, K.J., 2004. Discriminating between intra- and extracellular metals using chemical extractions. *Limnol. Oceanogr. Methods* 2, 237–247.
- Hogstrand, C., Verbost, P.M., Bonga, S.E., Wood, C.M., 1996. Mechanisms of zinc uptake in gills of freshwater rainbow trout: interplay with calcium transport. *Am. J. Physiol. Regul. Integr. Comp. Physiol.* 270, R1141–R1147.
- Iwasaki, Y., Kamo, M., Naito, W., 2015. Testing an application of a biotic ligand model to predict acute toxicity of metal mixtures to rainbow trout. *Environ. Toxicol. Chem.* 34, 754–760.
- Komjarova, I., Blust, R., 2009. Multimetal interactions between Cd, Cu, Ni, Pb, and Zn uptake from water in the zebrafish *Danio rerio*. *Environ. Sci. Technol.* 43, 7225–7229.
- Lavoie, M., Campbell, P.G.C., Fortin, C., 2012. Extending the biotic ligand model to account for positive and negative feedback interactions between cadmium and zinc in a freshwater alga. *Environ. Sci. Technol.* 46, 12129–12136.
- Meyer, J.S., Farley, K.J., Garman, E.R., 2015. Metal mixtures modeling evaluation project: 1. Background. *Environ. Toxicol. Chem.* 34, 726–740.
- Muysen, B.T.A., De Schampelaere, K.A.C., Janssen, C.R., 2006. Mechanisms of chronic waterborne Zn toxicity in *Daphnia magna*. *Aquat. Toxicol.* 77, 393–401.
- Niyogi, S., Wood, C.M., 2004. Biotic ligand model, a flexible tool for developing site-specific water quality guidelines for metals. *Environ. Sci. Technol.* 38, 6177–6192.
- Niyogi, S., Brix, K.V., Grosell, M., 2014. Effects of chronic waterborne nickel exposure on growth, ion homeostasis, acid-base balance, and nickel uptake in the freshwater pulmonate snail, *Lymnaea stagnalis*. *Aquat. Toxicol.* 150, 36–44.
- Niyogi, S., Nadella, S.R., Wood, C.M., 2015. Interactive effects of waterborne metals in binary mixtures on short-term gill-metal binding and ion uptake in rainbow trout (*Oncorhynchus mykiss*). *Aquat. Toxicol.* 165, 109–119.
- Norwood, W.P., Borgmann, U., Dixon, D.G., Wallace, A., 2003. Effects of metal mixtures on aquatic biota: a review of observations and methods. *Hum. Ecol. Risk Assess. Int. J.* 9, 795–811.
- Nys, C., Versieren, L., Cordery, K.I., Blust, R., Smolders, E., De Schampelaere, K.A.C., 2017. Systematic evaluation of chronic metal-mixture toxicity to three species and implications for risk assessment. *Environ. Sci. Technol.* 51, 4615–4623.
- Paquin, P.R., Gorsuch, J.W., Apte, S., Batley, G.E., Bowles, K.C., Campbell, P.G.C., Delos, C.G., Di Toro, D.M., Dwyer, R.L., Galvez, F., Gensemer, R.W., Goss, G.G., Hogstrand, C., Janssen, C.R., McGeer, J.C., Naddy, R.B., Playle, R.C., Santore, R.C., Schneider, U., Stubblefield, W.A., Wood, C.M., Wu, K.B., 2002. The biotic ligand model: a historical overview. *Comp. Biochem. Physiol. C: Toxicol. Pharmacol.* 133, 3–35.
- Pelgrom, S., Lamers, L., Lock, R., Balm, P., Bonga, S.W., 1995. Interactions between copper and cadmium modify metal organ distribution in mature tilapia, *Oreochromis mossambicus*. *Environ. Pollut.* 90, 415–423.
- Pyatt, F.B., Pyatt, A.J., Pentreath, V.W., 1997. Distribution of metals and accumulation of lead by different tissues in the freshwater snail *Lymnaea stagnalis* (L.). *Environ. Toxicol. Chem.* 16, 1393–1395.
- Pyatt, F.B., Metcalfe, M.R., Pyatt, A.J., 2003. Copper bioaccumulation by the freshwater snail *Lymnaea peregra*: a toxicological marker of environmental and human health? *Environ. Toxicol. Chem.* 22, 561–564.
- Rogers, J.T., Richards, J.G., Wood, C.M., 2003. Ionoregulatory disruption as the acute toxic mechanism for lead in the rainbow trout (*Oncorhynchus mykiss*). *Aquat. Toxicol.* 64, 215–234.
- Santore, R.C., Ryan, A.C., 2015. Development and application of a multimetal multibiotic ligand model for assessing aquatic toxicity of metal mixtures. *Environ. Toxicol. Chem.* 34, 777–787.
- Schlekat, C.E., Van Genderen, E., De Schampelaere, K.A.C., Antunes, P.M.C., Rogevich, E.C., Stubblefield, W.A., 2010. Cross-species extrapolation of chronic nickel biotic ligand models. *Sci. Total Environ.* 408, 6148–6157.
- Schlichter, L.C., 1982. Unstirred mucus layers: ion exchange properties and effect on ion regulation in *Lymnaea stagnalis*. *J. Exp. Biol.* 98, 363–372.
- Slaveykova, V.I., Wilkinson, K.J., 2002. Physicochemical aspects of lead bioaccumulation by *Chlorella vulgaris*. *Environ. Sci. Technol.* 36, 969–975.

- Tipping, E., Lofts, S., Sonke, J.E., 2011. Humic ion-binding model VII: a revised parameterisation of cation binding by humic substances. *Environ. Chem.* 8, 225–235.
- Unsworth, E.R., Warnken, K.W., Zhang, H., Davison, W., Black, F., Buffle, J., Cao, J., Clevén, R., Galceran, J., Gunkel, P., Kalis, E., Kistler, D., van Leeuwen, H.P., Martin, M., Noel, S., Nur, Y., Odzak, N., Puy, J., van Riemsdijk, W., Sigg, L., Temminghoff, E., Tercier-Waeber, M.-L., Toepperwien, S., Town, R.M., Weng, L., Xue, H., 2006. Model predictions of metal speciation in freshwaters compared to measurements by in situ techniques. *Environ. Sci. Technol.* 40, 1942–1949.
- Van Genderen, E., Adams, W., Dwyer, R., Garman, E., Gorsuch, J., 2015. Modeling and interpreting biological effects of mixtures in the environment: introduction to the metal mixture modeling evaluation project. *Environ. Toxicol. Chem.* 34, 721–725.
- Vijver, M.G., Elliott, E.G., Peijnenburg, W.J.G.M., de Snoo, G.R., 2011. Response predictions for organisms water-exposed to metal mixtures: a meta-analysis. *Environ. Toxicol. Chem.* 30, 1482–1487.
- Wood, C.M., 2001. Toxic responses of the gill. In: Schlenk, D., Benson, W.H. (Eds.), *Target Organ Toxicity in Marine and Freshwater Teleosts*. Taylor & Francis, London, UK, pp. 11–99.